

OPTICS AND SPECTROSCOPY

DIURNAL DYNAMICS OF STANDARD DEVIATIONS OF THREE WIND VELOCITY COMPONENTS IN THE ATMOSPHERIC BOUNDARY LAYER

L. G. Shamanaeva,^{1,2} N. P. Krasnenko,^{3,4} and O. F. Kapegesheva²

UDC 551.501.755 + 551.501.796

Diurnal dynamics of the standard deviation (SD) of three wind velocity components measured with a minisodar in the atmospheric boundary layer is analyzed. Statistical analysis of measurement data demonstrates that the SDs for x- and y-components σ_x and σ_y lie in the range from 0.2 to 4 m/s, and $\sigma_z = 0.1\text{--}1.2$ m/s. The increase of σ_x and σ_y with the altitude is described sufficiently well by a power law with exponent changing from 0.22 to 1.3 depending on time of day, and σ_z increases by a linear law. Approximation constants are determined and errors of their application are estimated. It is found that the maximal diurnal spread of SD values is 56% for σ_x and σ_y , and 94% for σ_z . The established physical laws and the obtained approximation constants allow the diurnal dynamics of the SDs for three wind velocity components in the atmospheric boundary layer to be determined and can be recommended for application in models of the atmospheric boundary layer.

Keywords: atmospheric boundary layer, acoustic sounding, sodar, wind velocity components, standard deviations, diurnal dynamics.

Information on the spatiotemporal dynamics of the wind velocity vector, its average value, and SDs of its components in the atmospheric boundary layer (ABL) is important from both fundamental and applied viewpoints [1–3]. It is necessary for a study of the dynamics of atmospheric processes, forecast of the air basin state, estimation of polluting impurity transfer, calculation of heat and momentum fluxes, construction of ABL models, meteorological weather forecast, and so on. Data on the statistical characteristics of wind velocity and, in particular, SD play an important role in calculations of constructional loads and development of communication and detection and ranging systems.

To obtain this data, for example, to measure the wind velocity in the ABL, it is expedient to use sodars (acoustic radars); a large number of works are devoted to this problem (for example, see [4–6]). Works on the wind velocity variance in the ABL are much less in number, and most of them, including [5, 7–9], study the altitude dependence of the variance of only the vertical wind velocity component. Naturally, this is insufficient. To fill the gap, in [10] the spatiotemporal dynamics of the wind velocity variance from the data of Doppler mini-sodar measurements [11] in the ABL was analyzed. The present work continues investigations in this direction and presents diurnal variations of the SDs of three wind velocity components $\sigma_x(z, t)$, $\sigma_y(z, t)$, and $\sigma_z(z, t)$ retrieved from minisodar measurements and their analytical approximation.

¹V. E. Zuev Institute of Atmospheric Optics of the Siberian Branch of the Russian Academy of Sciences, Tomsk, Russia, e-mail: sima@iao.ru; ²National Research Tomsk State University, Tomsk, Russia, e-mail: kapegesheva_o_o@mail.ru; ³Institute of Monitoring of Climatic and Ecological Systems of the Siberian Branch of the Russian Academy of Sciences, Tomsk, Russia, e-mail: krasnenko@imces.ru; ⁴Tomsk State University of Control Systems and Radio Electronics, Tomsk, Russia. Translated from *Izvestiya Vysshikh Uchebnykh Zavedenii, Fizika*, No. 12, pp. 156–160, December, 2017. Original article submitted May 30, 2017.

EXPERIMENTAL PROCEDURE AND DATA PROCESSING ALGORITHM

The standard deviations $\sigma_x(z, t)$, $\sigma_y(z, t)$, and $\sigma_z(z, t)$ were obtained within 24 hours from $t_{\text{init}} = 1$ (10:00, local time, on September, 16) to $t_{\text{fin}} = 25$ (10:00, local time on September, 17) from measurements with the minisodar having a working frequency of 4900 Hz, pulse duration of 60 ms, and pulse repetition period of 4 s. Radiation in one sounding cycle was transmitted sequentially in three directions – vertically and at the angles $\alpha = 14^\circ$ to the vertical in two mutually orthogonal planes. Results of minisodar measurements at altitudes in the range $z = 5\text{--}200$ m in strobes z_j , $j = 1, \dots, 40$, with vertical extension $\Delta z = 5$ m each were processed. The SDs were calculated from the formulas

$$\sigma_x(z_j, t_k) = \sqrt{\left\langle \left(V'_x(z_j, t_k) \right)^2 \right\rangle} = \frac{1}{N-1} \sqrt{\sum_{i=1}^N \left(V_{xij}(t_k) - \langle V_x(z_j, t_k) \rangle \right)^2}, \quad (1)$$

$$\sigma_y(z_j, t_k) = \sqrt{\left\langle \left(V'_y(z_j, t_k) \right)^2 \right\rangle} = \frac{1}{N-1} \sqrt{\sum_{i=1}^N \left(V_{yij}(t_k) - \langle V_y(z_j, t_k) \rangle \right)^2}, \quad (2)$$

$$\sigma_z(z_j, t_k) = \sqrt{\left\langle \left(V'_z(z_j, t_k) \right)^2 \right\rangle} = \frac{1}{N-1} \sqrt{\sum_{i=1}^N \left(V_{zij}(t_k) - \langle V_z(z_j, t_k) \rangle \right)^2}. \quad (3)$$

Here $V_{xij}(t_k)$, $V_{yij}(t_k)$, and $V_{zij}(t_k)$ are the wind velocity components in the j th strobe of the i th measurement in the k th series started at the moment of time t_k . The data of 25 hourly series of sodar measurements from 10:00, local time, on September 16, till 10:00, local time, on September 17 were processed.

RESULTS AND DISCUSSION

Figure 1 shows in vector representation [12] the spatiotemporal dynamics of the average horizontal wind velocity component $V_h(z_j, t_k)$ retrieved from minisodar measurements on September 16 and 17. It can be seen that on September 16, the wind was stronger, especially at the bottom of the 100-meter layer. The increase in the altitude of the V_h maximum from 45 m at 10:00, local time, to 100 m at 14:00 is traced. This is due to the ascent of the surface night temperature inversion. In the vertical profile of the horizontal wind velocity, the presence of such phenomenon, as the wind shear dangerous to aircrafts [3] is clearly observed. At 18:00, the southwest direction of the jet flow was changed to the northwest, the jet altitude first increased from 100 m at 20:00 to 125 m at 21:00, and then decreased to 75 m at 22:00. By 23:00, the wind direction changed to southeast, and the wind became less strong. At night from September 16 to September 17, $V_h(z_j, t_k)$ did not exceed 1 m/s, and the wind direction strongly changed with altitude. By 04:00, at the bottom of the 100-meter layer the increase in the horizontal wind, caused by rising of the surface temperature inversion, was traced. The irregular behavior of the wind velocity in the lower 20-meter layer can be explained by the roughness of the underlying surface and its non-uniform warming.

Figure 2 shows the diurnal behavior of the SDs for three wind velocity components retrieved from the data of minisodar measurements. The data of series of measurements with 3-hour intervals are presented. From the figure it can be seen that σ_x , σ_y , and σ_z increase with the altitude. Attention is drawn to the isotropy of the SDs for the x - and y -components of the wind velocity: their diurnal behavior and values coincide within the measurement errors, except for the surface layer of 5–20 m, where the effect of the underlying surface is significant [2]. From Fig. 2a and b it can be seen that σ_x and σ_y values lie in the range from 0.2 to 4 m/s, and $\sigma_z = 0.1\text{--}1.2$ m/s (Fig. 2c). Here σ_z values fast increase with altitude within the surface layer. For higher altitudes, the σ_z growth is slowed down. In this case, at altitudes $z_{\text{min}} = 5$ m and $z_{\text{max}} = 200$ m, the minimal SD values $\sigma_{x\text{min}} = 0.7\text{--}2.8$ m/s and $\sigma_{y\text{min}} = 0.7\text{--}3.3$ m/s were observed at 13:00, and their maximum values $\sigma_{x\text{max}} = 1.4\text{--}3.6$ m/s and $\sigma_{y\text{max}} = 1.6\text{--}3.4$ m/s at these altitudes were observed at 07:00; $\sigma_{z\text{min}} = 0.1\text{--}0.5$ m/s were observed at 13:00, and $\sigma_{z\text{max}} = 0.5\text{--}1.1$ m/s were observed at 01:00. In this case, the maximum

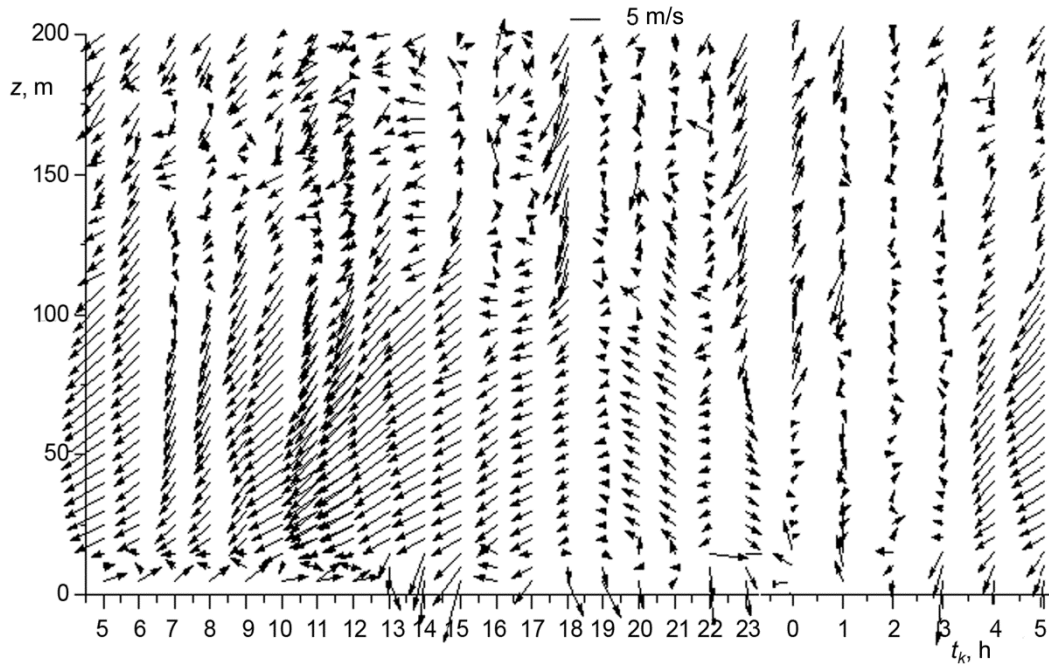


Fig. 1. Hourly spatiotemporal dynamics of the horizontal wind in the vector representation from the results of minisodar measurements on September, 16 and 17. Orientation: the north is at the top, and the west is on the left.

spread of the SD values at these altitudes, calculated from the formula $\Delta\sigma_i(z) = \frac{\sigma_{i\max}(z) - \sigma_{i\min}(z)}{\sigma_{i\max}(z)} \cdot 100\%$, reached 56% for $\sigma_{x,y}(z)$ and 94% for $\sigma_z(z)$. Our statistical analysis of the diurnal dynamics of the measured vertical SD profiles demonstrated that the increase of $\sigma_x(z, t)$ and $\sigma_y(z, t)$ with altitude is described by power-law dependences, and $\sigma_z(z, t)$ linearly depends on the altitude:

$$\tilde{\sigma}_x(z, t) = C_1(t)z^{N_1(t)}, \quad (4)$$

$$\tilde{\sigma}_y(z, t) = C_2(t)z^{N_2(t)}, \quad (5)$$

$$\tilde{\sigma}_z(z, t) = A(t) + B(t)z. \quad (6)$$

The corresponding approximation constants are shown in Fig. 3. The approximation errors estimated from values of their standard deviations $\tilde{\sigma}_x(z, t)$, $\tilde{\sigma}_y(z, t)$, and $\tilde{\sigma}_z(z, t)$ from the measured values, were in the intervals 0.015–0.045, 0.011–0.051, and 0.0031–0.0048 m/s, respectively.

From Fig. 3 it can be seen that the approximation constants for $\tilde{\sigma}_x(z, t)$ and $\tilde{\sigma}_y(z, t)$ change synchronously during the day, demonstrating the general tendency toward their decrease with increase in the measurement time, and their values practically coincide within the approximation errors. This confirms the conclusion about their isotropy. In addition, two local minima at $t_1 = 15$ h and $t_2 = 23$ h are clearly seen on the diurnal course of $N_1(t)$ and $N_2(t)$. Their occurrence is accompanied by the increasing altitude dependence of the SDs, practically to linear one at 23:00, when the exponents $C_1(t_2)$ and $C_2(t_2)$ approach to 1 (see formulas (4) and (5)). As to the altitude dependence of the SD profiles determined by the coefficients $C_1(t)$ and $C_2(t)$, from Fig. 3a it can be seen that from 10:00 till 14:00, the SDs are

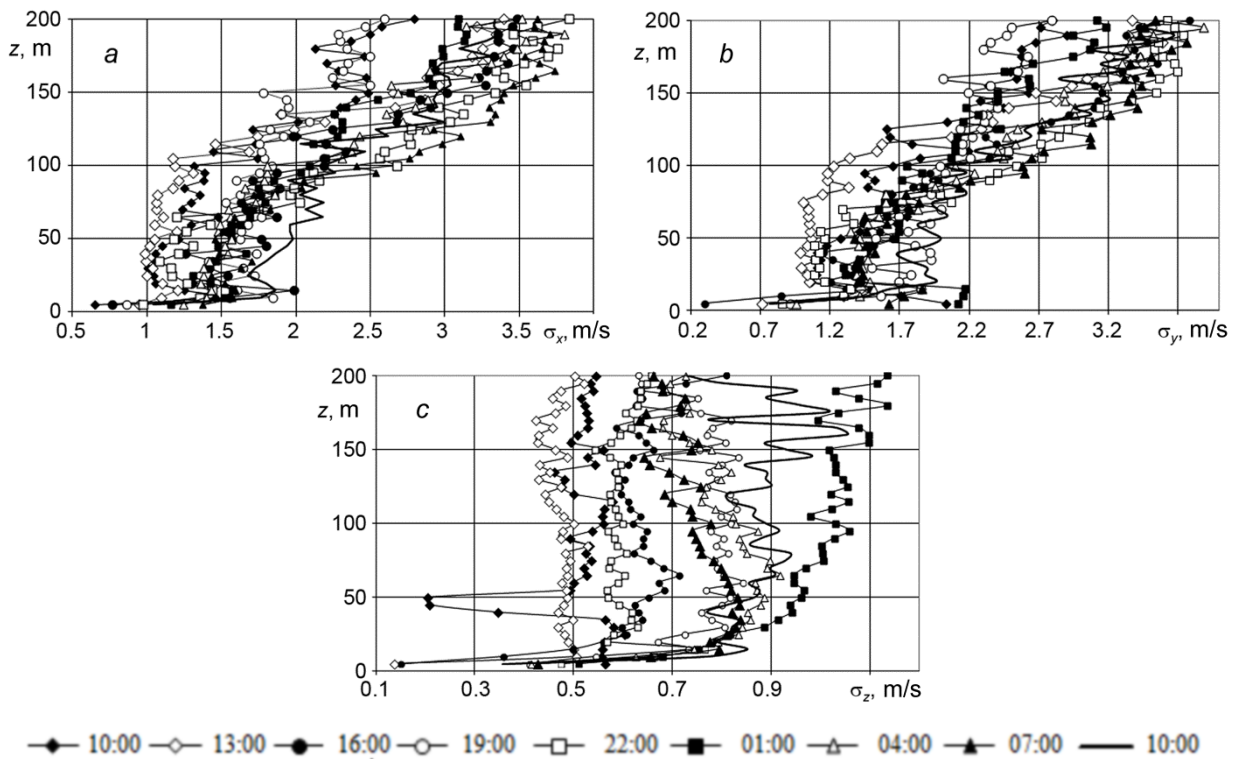


Fig. 2. Diurnal dynamics of the SDs for three wind velocity components retrieved from the data of minisodar measurements on September 16–17. Time of the beginning of each series of measurements with 3-hour intervals between the series is indicated under the figure.

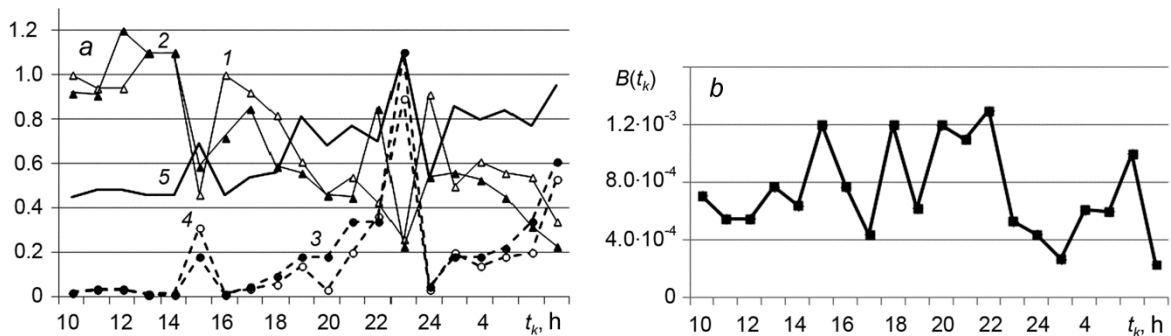


Fig. 3. Approximation constants of the diurnal behavior of the SDs for three wind velocity components in formulas (4)– (6): *a*) approximation constants $N_1(t_k)$ (curve 1), $N_2(t_k)$ (curve 2), $C_1(t_k)$ (curve 3), $C_2(t_k)$ (curve 4), $A(t_k)$ (curve 5), and $B(t_k)$ (curve 6).

practically independent of the altitude, then from 14:00 till 16:00 they increase with altitude as $\sim z^{0.2}$, and from 16:00 till 23:00 the altitude dependence increases practically to a linear one. At 24:00, $C_1(t)$ and $C_2(t)$ decrease practically down to 0. From 01:00, they increase again to 0.6. Thus, from the data shown in Fig. 3*a*, it is possible to draw the conclusion about semidiurnal dynamics of the SDs for the *x*- and *y*-components of the wind velocity and about the presence of two local minima at 15:00 and 23:00.

For $\tilde{\sigma}_z(z, t)$ a linear growth with altitude (see formula (6)) was characteristic, with the proportionality coefficient $B(t)$, shown in Fig. 3b. Moreover, the surface SD values for the z -component of wind velocity (curve 5 in Fig. 3a) increase from 0.4 to 0.9 m/s when the observation time increased; they have two local maxima at 15:00 and 23:00.

CONCLUSIONS

Our analysis of the diurnal dynamics of vertical SD profiles for three wind velocity components has demonstrated that the growth of $\sigma_x(z, t)$ and $\sigma_y(z, t)$ with altitude z is well described by the power-law dependences, and $\sigma_z(z, t)$ increases with z following the linear dependence. The SD approximation constants were determined and the errors of their application were estimated. The maximal diurnal spread of σ_x and σ_y was 56%; for σ_z , it was 94%. The established physical regularities and the obtained approximation constants allow the altitude and diurnal dynamics of the SDs for three wind velocity components to be described and can be recommended for application in ABL models.

This work was supported in part by the Assignment of the Ministry of Education and Science of the Russian Federation (Project No. 5.3279.2017/4.6) and by the Siberian Branch of the Russian Academy of Sciences (Project of Fundamental Research No. IX.138.2.5).

REFERENCES

1. N. L. Byzova, V. I. Ivanov, and E. K. Garger, Turbulence in the Atmospheric Boundary Layer [in Russian], Gidrometeoizdat, Leningrad (1989).
2. Atmosphere: A Handbook [in Russian], Gidrometeoizdat, Leningrad (1991).
3. P. D. Astapenko, A. M. Baranov, and I. M. Shvarev, Aviation Meteorology [in Russian], Transport, Moscow (1985).
4. R. L. Coulter and M. A. Kallistratova, Meteorol. Atm. Phys., **85**, Nos. 1–2, 3–19 (2004).
5. R. L. Coulter, in: Proc. 11th ISARS, Rome (2002), pp. 321–327.
6. S. Bradley, Atmospheric Acoustic Remote Sensing: Principles and Applications, CRC Press Taylor & Francis Group, Boca; London; New York (2007).
7. S. Emeis, K. Baumann-Stanzer, M. Piringer, *et al.*, Meteorol. Z., **16**, No. 4, 393–406 (2007).
8. M. A. Lokoshchenko, V. G. Perepelkin, and N. V. Semenova, Meteorol. Z., **16**, No. 4, 407–417 (2007).
9. M. A. Lokoshchenko, V. G. Perepelkin, N. F. Elanskii, and I. A. Korneva, in: Proc. 15th ISARS, Paris (2010), Poster PME/14 (4 pp.).
10. O. F. Kapegesheva, N. P. Krasnenko, M. V. Tarasenkov, and L. G. Shamanaeva, Proc. SPIE, **9680**, 96804E-1–96804E-4 (2015); DOI: 10/1117/12.2205801.
11. <http://minisodar.org>.
12. N. P. Krasnenko, M. V. Tarasenkov, and L. G. Shamanaeva, Russ. Phys. J., **57**, No. 11, 1539–1546 (2014).